

# Control-A-Video: Controllable Text-to-Video Generation with Diffusion Models

Weifeng Chen,<sup>\*</sup> Yatai Ji,<sup>\*</sup> Jie Wu, Hefeng Wu,<sup>†</sup> Pan Xie,  
 Jiashi Li, Xin Xia, Xuefeng Xiao, Liang Lin  
 Project Page: <https://controlavideo.github.io>

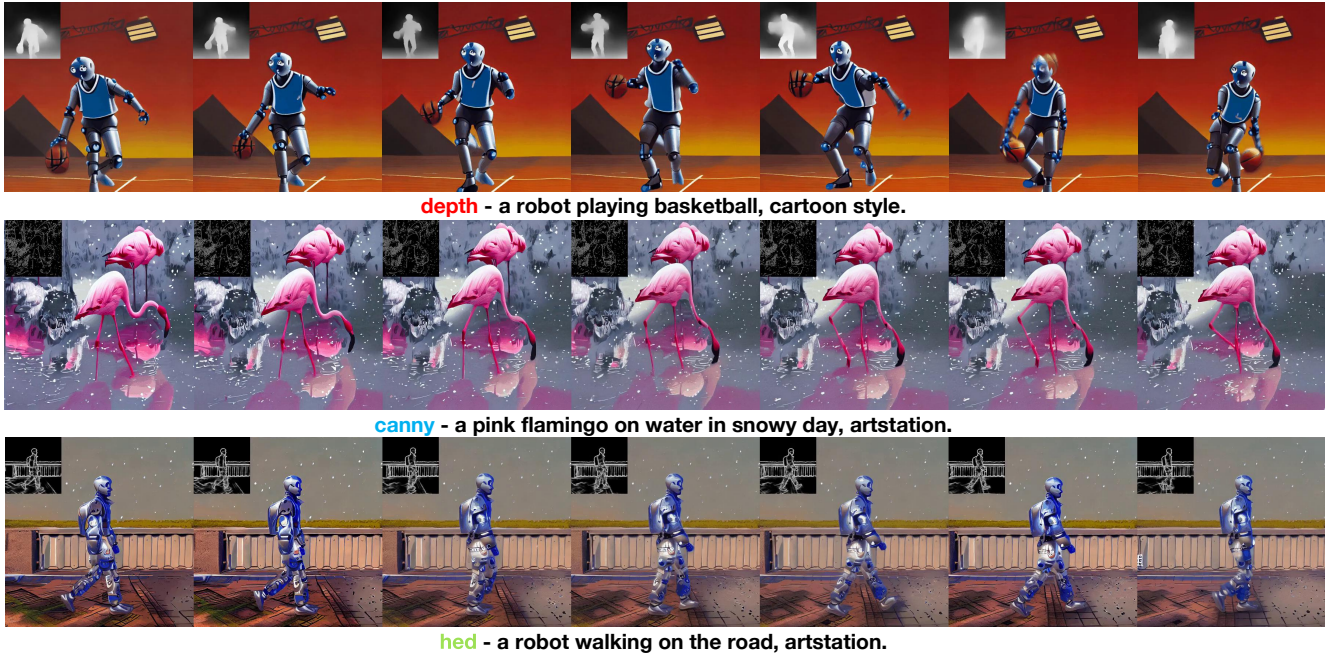


Figure 1. Our model generates high-quality and consistent videos conditioned on a text prompt and additional control maps, such as **depth maps** (first row), **canny edge maps** (second row), **hed edge maps** (third row).

## Abstract

Recent advancements in diffusion models have unlocked unprecedented abilities in visual creation. However, current text-to-video generation models struggle with the trade-off among movement range, action coherence and object consistency. To mitigate this issue, we present a controllable text-to-video (T2V) diffusion model, called Control-A-Video, capable of maintaining consistency while customizable video synthesis. Based on a pre-trained conditional text-to-image (T2I) diffusion model, our model aims to generate videos conditioned on a sequence of control signals, such as edge or depth maps. For the purpose of improving object consistency, Control-A-Video integrates motion priors and content priors into video generation. We propose two motion-adaptive noise initialization strategies, which

are based on pixel residual and optical flow, to introduce motion priors from input videos, producing more coherent videos. Moreover, a first-frame conditioned controller is proposed to generate videos from content priors of the first frame, which facilitates the semantic alignment with text and allows longer video generation in an auto-regressive manner. With the proposed architecture and strategies, our model achieves resource-efficient convergence and generate consistent and coherent videos with fine-grained control. Extensive experiments demonstrate its success in various video generative tasks such as video editing and video style transfer, outperforming previous methods in terms of consistency and quality.

## 1. Introduction

In recent years, there has been a rapid development in text-based visual content generation. Driven by the progress of

<sup>\*</sup>Equal contribution.

<sup>†</sup>Corresponding Author.

diffusion-based models, text-to-image synthesis [23, 27, 30] has made a tremendous breakthrough, which have demonstrated an impressive ability to generate high-quality images based on user-provided text prompts. Built on pre-trained T2I models, there is a surging interest in text-to-video synthesis in zero-shot manner [17, 26, 41] or training on large-scale video-text datasets [1, 4]. However, movement generation across video frames remains a formidable challenge.

A satisfactory generated video should fulfill three criteria: 1) a distinct range of movement, 2) coherent action during inter-frame transitions, 3) consistent appearance of objects in different frames without flickers. The current T2V models tend to generate videos with limited movement range due to the trade-off among movement range, action coherence and object consistency, as shown in Figure 2(a). When the motion range is large, consistency and coherence are difficult to maintain. To enhance video movements, the introduction of control signals during video generation is a potential solution. Controllable video synthesis [37, 40] allows users to specify desired contents and motions, realizing customized video generation with fine-grained control. Nevertheless, despite achieving controllable movements and coherent action, a notable challenge remains in ensuring object consistency. For instance, Figure 2(b) depicts that the appearance of horse changes across frames, although the motion is correct.

To address the issue, this paper presents a controllable T2V model, namely Control-A-Video, capable of maintaining consistency and coherence while customizable video synthesis. Specifically, Control-A-Video is designed to generate videos based on text and reference control maps, such as edge, depth or optical flow maps. In terms of model architecture, we develop our video generative model by reorganizing a pre-trained controllable T2I model [42], incorporating additional trainable temporal layers, and utilizing a spatial-temporal self-attention mechanism that facilitates fine-grained interactions between frames. Furthermore, we propose some novel strategies to introduce motion priors and content priors, boosting object consistency.

The motion priors come from two types of pioneering noise initialization approaches. The first method is to initialize noise based on pixel residual between frames of the source video. The second one is to calculate the initial noise of next frame based on optical flow of the source video movement. Inspired by [6], these approaches can make the initial distribution of noise latents more reasonable, enhancing relevance among frame latents and improving video consistency. By leveraging motion priors, the Control-A-Video is able to closely resemble motion changes in the reference video and produce coherent videos that are less flickering.



Figure 2. The prompt for generation is “magical flying horse with a man jumping over an obstacle, artstation”. (a) Text-to-video model<sup>1</sup>, (b) Controllable text-to-video baseline<sup>2</sup>, (c) Our Control-A-Video model. The result from text-to-video model<sup>1</sup> has only a limited movement range. Baseline controllable generation<sup>2</sup> can create videos with desired movements under the control signals, but it loses consistency. In contrast, our model is capable of maintaining object consistency in customizable video synthesis.

For the content priors, instead of training models to directly generate entire videos, we introduce an innovative training scheme that produces video predicated on the initial frame. With such a straightforward yet effective strategy, it becomes more manageable to disentangle content and temporal modeling. Our model only needs to learn how to generate subsequent frames with content priors of the first frame, inheriting generative capabilities from the image domain and facilitating consistency with objects in the first frame. During inference, we generate the first frame conditioned on the control map of the first frame and a text prompt. Then, we generate subsequent frames conditioned on the first frame, text, and subsequent control maps. In the two-stage generation, the first frame produced in text-to-image process contains more accurate semantics with text, promoting cross-modal alignment of the video. Meanwhile, another benefit of such strategy is that our model can auto-regressively generate a longer video by treating the last frame of the previous iteration as the initial frame.

With the above strategies, controllable generation results have better consistency like in Figure 2(c). Moreover, our model is easy to converge with fewer training resources, e.g., our iteration samples are 1.6M compared to 115M in Gen-1’s [4].

In a nutshell, we propose Control-A-Video, a controllable T2V diffusion model, which has the following advantages: (i) Our model is able to generate text-guided videos conditioned on various types of control maps, enhancing the movement range and action coherence in text-to-video synthesis. (ii) We introduce pixel residual-based and opti-

<sup>1</sup>We use the api on <https://www.genmo.ai/>.

<sup>2</sup>We train the baseline with only depth map condition.

cal flow-based noise initialization strategies, that incorporate motion priors from the reference videos to promote relevance among frame latents, making videos more consistent and less flickering. (iii) To achieve further object consistency, we also present a novel first-frame conditioned controller to introduce content priors. Our model generates videos based on semantics of the initial frame, transferring text-aligned knowledge from images to videos. As a byproduct of the first-frame conditioning strategy, Control-A-Video can auto-regressively generate longer videos. (iv) Through our proposed approaches, experiments demonstrate that our framework is capable of generating higher-quality, consistent videos using fewer training resources.

## 2. Related Work

### 2.1. Text-to-image generation with diffusion models

Over the past few years, there have been significant advancements in the field of image generation, particularly with the Denoising Diffusion Probabilistic Model [13, 33]. This model has demonstrated impressive capabilities, surpassing the performance of Generative Adversarial Networks (GANs) [8] and Variational Autoencoders (VAEs) [18]. To generate images conditioned on text, several approaches have been proposed, such as GLIDE [23], DALLE-2 [27], Imagen [30], and LDMs [27]. These models train diffusion models using large-scale text-image pairs, enabling the generation of images with text conditions. To enhance control in image generation, few-shot tuning methods like Textual Inversion [5] and Dreambooth [29] have been developed for personalized generation. Editing techniques Prompt2Prompt [11], Plug-and-Play [34], and InstructPix2Pix [2] offer methods to edit and refine the generated images. Notably, approaches such as ControlNet [42], T2I-Adapter [21], and Composer [16] focus on fine-tuning T2I model with condition-text-image pairs, enabling the integration of control hints such as edges, poses, and depth maps. In this paper, we adopt a similar idea to ControlNet and extend it to the domain of video generation with conditions. By leveraging the advancements made in T2I models, we are able to generate videos of consistency and diversity.

### 2.2. Text-to-video generation with diffusion models

The remarkable accomplishments of diffusion models in Text-to-Image (T2I) generation have inspired researchers to venture into the field of video generation. Several notable advancements, including VDM [15], Imagen Video [14], Make-A-Video [32] and Animatediff [9], extend text-to-image diffusion models by training them on extensive text-video pairs. To overcome the challenge of generating longer videos, LVDM [10], MCVD [35], and Align-Your-Latents [1] adopt an auto-regressive approach, sequentially generating video frames to ensure temporal co-

herence and continuity. For text-based video translation, zero-shot methods such as Text2Video-Zero [17], FateZero [26], Vid2VidZero [36], and Video-P2P [20], explore the latent space of diffusion models and employ temporal attention mechanisms to generate videos. However, a challenge faced by these methods is the potential lack of temporal consistency. To improve the consistency of the generated videos, flow-based approaches like Render-A-Video [41] and TokenFlow [7] propose to introduce flow constraints in diffusion process. On the other hand, tuning-based methods, such as Tune-A-Video [38] and CodeF [24], achieve better consistency by fine-tuning the models in the inference stage, albeit requiring an additional tuning process. Furthermore, Gen-1 [4] and VideoCompose [37] propose to train video diffusion models with additional conditional maps. In comparison to these existing approaches, this paper presents a novel two-stage generation approach and employs a noise manipulation strategy to achieve enhanced temporal consistency in text-based video translation.

## 3. Method

In this section, we will introduce the structure and strategies of our text-to-video model. The preliminary knowledge about LDMs [13] and ControlNet [42] can be found in supplementary material. Our model incorporates motion layers and operations to enable effective temporal modeling. Afterwards, we propose a novel motion-aware noise initialization approach that serves as a video prior for ensuring consistent video generation. This approach includes two types of noise: pixel residual-based and optical flow-based noise. The residual-based noise captures the subtle variations in video frames, while the flow-based noise models the motion dynamics between frames. Furthermore, we provide a detailed overview of the training procedure and inference pipeline of our text-to-video model by involving generating the first frame as a precursor and utilizing it as a conditioning factor for video generation.

### 3.1. Model Architecture

Building upon a controllable T2I model [42], we introduce two architectural refinements for video generation: (i) To enable effective temporal modeling, we incorporate an additional temporal layer following each 2-dimensional (2D) layer, such as convolution and attention layers. (ii) To further enhance frame modeling, we employ a spatial-temporal self-attention mechanism. This approach draws inspiration from zero-shot methods like vid2vid-zero [36], where spatial and temporal relationships are jointly modeled to capture dependencies across frames.

In Figure 3, each frame’s features are processed through either a 2D convolution layer or a spatial attention layer. Subsequently, these frame-level features are collectively passed to a trainable 1D convolutional layer or tempo-



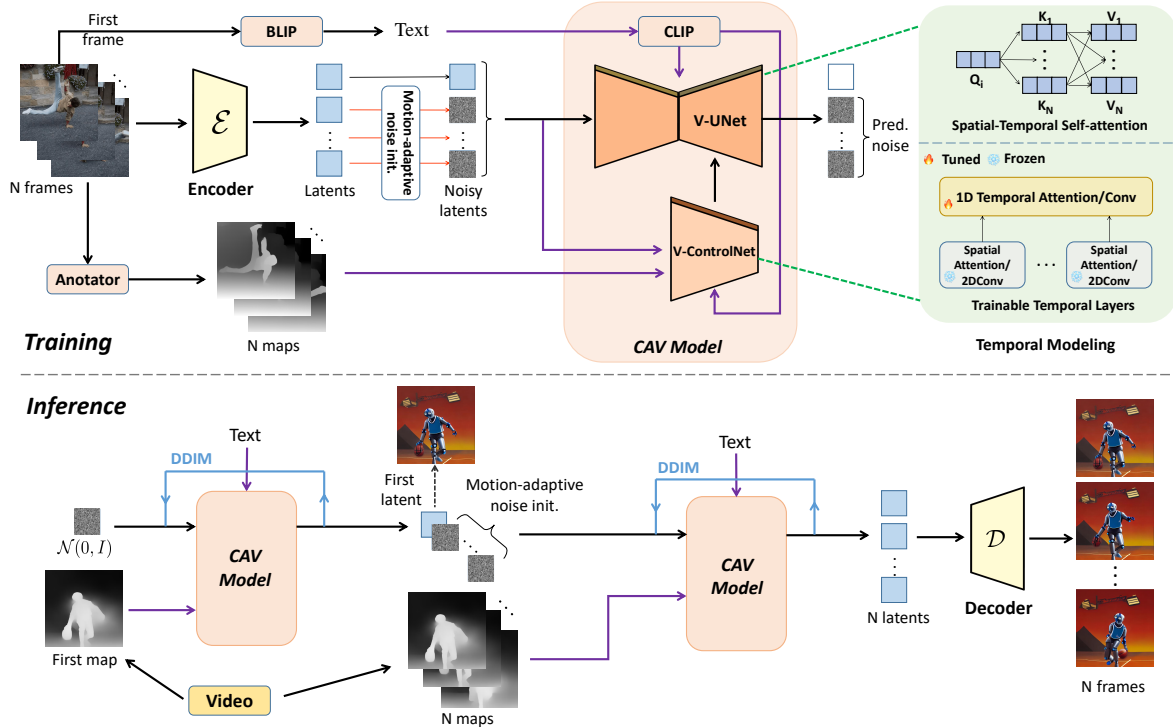


Figure 3. Illustration of our Control-A-Video pipeline. **Model Architecture:** We apply spatial-temporal self-attention and trainable temporal layers to both the image UNet and the image ControlNet, enabling the model to generate videos. **Training:** The model input includes video and its text prompt from BLIP captioning [19] and control maps from an annotator (e.g. depth estimation model). Each frame is passed to the encoder to get the latent code. We add noise with motion priors to each latent except for the first frame and train the model to predict the subsequent noise conditioned on the first frame. **Inference:** After training, our model is able to generate the first frame conditioned on its control map. The generated first frame is then used to generate subsequent frames with the content priors.

ral attention for frame modeling. Moreover, to enable fine-grained modeling, we adapt the spatial self-attention mechanism by incorporating spatial-temporal self-attention across frames, which can be formulated as:

$$\text{SelfAttn}(Q, K, V) = \text{Softmax}\left(\frac{QK^T}{\sqrt{d}}\right)V, \quad (1)$$

$$Q = W^Q \bar{v}_i, K = W^K [\bar{v}_0, \dots, \bar{v}_{N-1}], V = W^V [\bar{v}_0, \dots, \bar{v}_{N-1}] \quad (2)$$

where  $\bar{v}_i$  denotes the token sequence of frame  $i$ , and  $[\bar{v}_0, \dots, \bar{v}_{N-1}]$  denotes the concatenation of the  $N$  frames. As shown in Eq. 2, we concatenate features  $K, V$  of  $N$  frames so that each position has a global perception of all video frames and tends to generate more consistent results.

### 3.2. Motion-adaptive Noise Initializer

The diffusion model aims to denoise a signal by learning from Gaussian noise, where different initial noise samples can yield different results. In our study, we leverage the components of T2I models for video generation and observe that the latent spaces of consecutive video frames exhibit high correlation. In Figure 4, we can see that consec-

utive frames (represented by red points) are close to each other. However, when we add per-frame typical Gaussian noise (represented by green points) to each frame, we observe that the distribution between frames is disrupted. Not only does the distance between frames increase, but the overall distribution across frames also becomes distorted. Motivated by these findings, we propose a strategy to incorporate motion into the noise initialization process, aiming to align the noise closer to the video frames. To achieve this, we introduce two types of motion priors for video generation: flow-based and residual-based. By integrating motion-based noise into the latent space of the video, we empirically observe that the distribution of each frame maintains its similarity and coherence. As depicted in Figure 4, the distribution of the flow-based noise (represented by orange points) is most similar to the original video, while the residual-based noise (represented by pink points) also exhibits high correlation. Intuitively, learning to reconstruct the video from motion-based noise is more feasible compared to using Gaussian noise since the latent similarity is preserved. Specifically, the proposed algorithm is outlined in Algorithm 1.

**Residual-based Noise Prior:** To maintain consistent



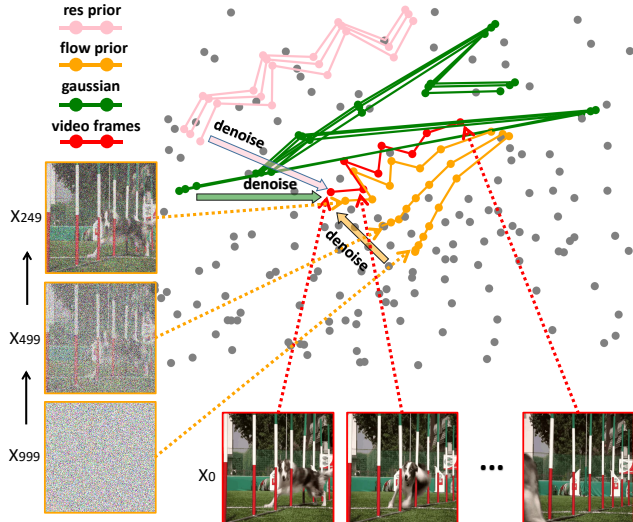


Figure 4. **Motion-adaptive Noise Prior**: we visualize the t-SNE plot of the noisy latents of video frames. The red one denotes the video  $X_0$ , which is the end of denoising process and we gradually add noise at different timesteps (249, 499, 999) to get its noise maps. The pink one is residual noise, the orange one is flow noise, the green one is gaussian noise. There’re two findings in this map: (1) Two adjacent frames are the most similar, so a sequence of frames should be linked with a line. (2) For gaussian noise, the “line” relation is distorted and each dot become away from the origin video; for flow-based noise and residual-based noise, the “line” is still parallel to the origin frames and the distance is not far away the  $X_0$ .

noise in static regions and introduce varying noise in moving regions, we employ a residual-based noise prior. By computing the residual between consecutive frames, we initialize the noise distribution accordingly after downsampling. This approach ensures that unchanged areas exhibit the same noise, while changing areas possess distinct noise patterns. Additionally, a threshold is utilized to differentiate static and dynamic regions, providing control over the smoothness of the generated videos.

**Flow-based Noise Prior**: In order to align the generated video’s flow with the motion depicted in the frames, we introduce a flow-based noise prior. This involves computing the optical flow between consecutive frames in pixel space, followed by downsampling the flow information to the latent space. By propagating the flow through subsequent noise latents, we align the noise patterns with the expected motion flow, resulting in visually coherent and realistic videos.

### 3.3. Latent First-frame Conditioned Controller

**During Training**: A naive approach for temporal learning in a video diffusion model would be to train the model to predict the entire video sequence. However, this would require a large amount of video data to learn the diversity that

---

#### Algorithm 1: Motion-adaptive Noise Propagation

---

```

1 Initialize noise  $x$  with  $N$  frames,
    $x^n \leftarrow \mathcal{N}(0, I), n = 0, \dots, (N - 1)$ 
2 Given InputVideo :  $v = [v^n, n = 0, \dots, (N - 1)]$ 
3  $R_{thres}$  : The threshold for residual change
4  $DownSample()$  : Resize to align the size of noise
5 —
6 residual-based
7 for  $i$  from 1 to  $N$  do
8    $res = norm(v^i - v^{(i-1)})$ 
9    $res_{mask} = res > R_{thres}$ 
10   $res_{mask} = DownSample(res_{mask})$ 
11   $x^i = [x^i - x^{(i-1)}] * res_{mask} + x^{(i-1)}$ 
12 end
13 —
14 flow-based
15 for  $i$  from 1 to  $N$  do
16    $flow_{pixel}^i = flow(v^i, v^{(i-1)})$ 
17    $flow_{latent}^i = DownSample(flow_{pixel}^i)$ 
18    $x^i = GridSample(x^{(i-1)}, flow_{latent}^i)$ 
19 end

```

---

has already presented in the image domain. To enhance the effectiveness of model training, we propose a first-frame latent conditioning method that generates video sequences conditioned on content priors of the first frame. This approach reduces the need for the model to memorize video content in the training set and instead focuses on learning to reconstruct motion, which makes it possible to achieve better results with fewer training resources. As shown in Figure 3, during training, we add noise to each frames except the first, so the model learns to generate subsequent frames based on the first frame  $v^1$ . Thus the loss function can be formulated as:

$$min_{\theta} ||\epsilon - \epsilon_{\theta}(x_t, t, c_p, c_f, \mathcal{E}(v^1))||_2^2 \quad (3)$$

By adopting this approach, our model can effectively utilize the motion information from the control maps and follow the content from the first frame. This simple yet effective strategy not only allows our model to generalize the domain from image to video, but also to auto-regressively generate longer videos.

**During Inference**: We generate the initial frame, denoted as  $v^1$ , by providing the model with Gaussian noise in the form of a single frame  $x^1$  along with conditioning factors including a text prompt  $c_p$  and a first frame control map  $c_f^1$ .

$$v^1 = ControlT2I(x^1, c_p, c_f^1) \quad (4)$$

Once we obtain the first frame  $v^1$  of the video, we generate the following frames conditioned on its latent code



Figure 5. **Auto-Regressive Generation:** Our model is able to generate long videos auto-regressively. The first row corresponds to the initial iteration, the second row is generated conditioned on the last frame of the first iteration, and so on for the third iteration.

$\mathcal{E}(v^1)$ :

$$v = \text{ControlT2V}(x, c_p, c_f, \mathcal{E}(v^1)) \quad (5)$$

With our proposed method of first-frame conditioning, our model is capable of generating video sequences with greater diversity than what is present in the training data. Additionally, our model has a distinct advantage in creating longer videos by utilizing previously generated frames as the initial frame in the subsequent iteration. This allows us to use an auto-regressive approach to produce videos of any length, which sets us apart from other video diffusion models that are limited to generating videos only once.

**Classifier-Free Guidance:** Classifier-free guidance [12] with a guidance scale  $\omega_t$  to sample the noise can be formulated as:

$$\begin{aligned} \hat{\epsilon}_\theta(x_t, t, c_p, c_f) &= \epsilon_\theta(x_t, t, \emptyset, c_f) \\ &+ \omega_t(\epsilon_\theta(x_t, t, c_p, c_f) - \epsilon_\theta(x_t, t, \emptyset, c_f)) \end{aligned} \quad (6)$$

where  $\emptyset$  denotes a null-text prompt, and  $\epsilon_\theta(x_t, t, \emptyset, c_f)$  represents negative representation. Based on this, we incorporate a sampling strategy in [4] that treats noise prediction of video generated frame-by-frame as a negative representation needed to be avoided. Consequently, the final prediction of noise is calculated as:

$$\begin{aligned} \hat{\epsilon}_\theta(x_t, t, c_p, c_f) &= \epsilon_{\theta I}(x_t, t, \emptyset, c_f) \\ &+ \omega_v(\epsilon_\theta(x_t, t, \emptyset, c_f) - \epsilon_{\theta I}(x_t, t, \emptyset, c_f)) \quad (7) \\ &+ \omega_t(\epsilon_\theta(x_t, t, c_p, c_f) - \epsilon_\theta(x_t, t, \emptyset, c_f)) \end{aligned}$$

Here,  $\omega_v$  denotes the scale of video guidance, and  $\epsilon_{\theta I}(x_t, t, \emptyset, c_f)$  denotes the prediction that each video frame is independently predicted. Just as a larger  $w_t$  can enhance text guidance, a larger  $w_v$  will result in a smoother overall effect.



Figure 6. **Qualitative Comparison:** We choose a hard case of a fast moving dog. Compared to other video editing and controllable generation models, our model exhibits high-quality and consistent results. (a) Input video, (b) Gen-1, (c) Text2Video-Zero, (d) Tokenflow, (e) Rerender A Video, (f) Videocomposer-imgcond, (g) Videocomposer-w/o imgcond, (h) Ours.

## 4. Experiments

### 4.1. Implementation Details

**DataSet Settings:** 100k video clips sourced from the Internet and 100k image-text pairs obtained from Laion [31].

**Training Settings:** Our model is initialized with pre-trained weights from Stable Diffusion v1.5 [27] and ControlNet [42]. We only train the temporal layers with an 8:2 ratio of video to image rate. The resolution is set to  $512 \times 512$ , the batch size to 16, the learning rate to  $10^{-5}$ , and the total number of training steps to  $10k$ . The model is evaluated using three control types: canny edge maps [3], hed edge maps [39], and depth maps.[28].

**Inference Settings:** The noise initialization threshold is set to 0.1, the scale for text guidance is 10.0, the scale for video guidance is 1.5, and DDIM uses 20 sampling steps.



## 4.2. Main Results

### 4.2.1 Controllable Video Generation

We showcase three types of controls extracted from video to demonstrate our system’s capacity to generate videos conditioned on various control types, as shown in Figure 1 and more results in supplementary material. Through experimentation, we found that depth maps provide less structural information than edge maps, resulting in more diverse video outputs. Edge maps, on the other hand, produce videos with enhanced details but a lesser degree of variability. For instance, in the first row of Figure 1, we transform a human into a cartoon robot using depth map control. In contrast, using edge maps in the third row still results in a human-robot transformation, but with more intricate details retained, such as the clothing pattern.

### 4.2.2 Auto-Regressive Long Video Generation

As illustrated in Section 3.3, we present the outcomes of auto-regressive video generation in Figure 5. The source video consists of 24 frames, and our objective is to convert a city at sunset into a frozen city. We generate the edited video through three iterations, each comprising eight frames. The subsequent video clips are produced auto-regressively based on the last frame of the previous iteration. The generated video exhibits consistency across various iterations, which attests to the efficacy of our first-frame conditioning approach.

### 4.2.3 Qualitative Analysis

Control-A-Video can incorporate various control signals, such as depth and optical flow maps, enabling it to naturally generalize to video editing and video style transfer. We conduct qualitative comparison on video editing with other models, including the editing model Gen-1 [4], Text2Video-Zero [17], Tokenflow [7], Rerender A Video [41], and the controllable generation model Videocomposer [37]. These models have similar settings for generating videos with additional controls. To demonstrate the superior performance of our model compared to others, we choose videos with significant movement ranges to evaluate, which are difficult to generate.

As shown in Figure 6, the first row depicts the original video, from which we extract depth maps and use a prompt ‘a dog running through a field of poles, van goah style painting’ to create a style transfer video. In the second row, although the result of Gen-1 has correct style, the generated dog is confused and lack details. The third row exhibits the result of Text2Video-Zero, which fails to produce a normal dog in the first three frames. The similar problem can also be found in Rerender-A-Video. In the result of Tokenflow, the dog is blurry and its style is unrelated. As for



Figure 7. Qualitative ablation study of the motion-adaptive noise initializer. (a) Input video, (b) Random, (c) Residual-based, (d) Flow-based.

Videocomposer, we generate the video with or without an extra style image, which helps model understand ‘van goah’ style. However, Videocomposer can’t maintain consistency of the dog in both situations. In the last row, we present the video generated by our model, which is most clear, consistent and text-aligned. More Comparison will be shown in supplementary material.

## 4.3. Ablation Studies

We conduct empirical ablation experiments on our proposed strategies to demonstrate the effectiveness of motion priors and content priors. We adopt depth maps from 20 video clips from Davis [25] and in-the-wild videos, which are used to generate videos based on a given text prompt. To evaluate text alignment, we calculate the cosine similarity between video embeddings of the output videos and text embeddings of the given prompts with X-CLIP [22]. To assess semantic consistency between different frames, we measure the similarities for frame CLIP embeddings of output videos. Furthermore, we compute the depth map errors and optical flow map errors between input and output videos, which reflect consistency on structure and movement respectively.

### 4.3.1 Motion-adaptive Noise Initializer

To demonstrate that pixel residual-based and optical flow-based noise initialization (simplify as RNI and FNI) strategies boost object consistency of videos, we perform visualization case study and quantitative comparison. Figure 7 illustrates the effect of different noise initialization strategies. In the second row, the bear has artifacts and distortion due to the lack of noise initialization. In contrast, the last





Figure 8. Ablation Study of Different Thresholds

two rows both exhibit consistent videos, and the video result of FNI has a better performance on color maintaining. As summarized in Table 1, both noise initialization methods improve all metrics over baseline. Especially in term of optical flow map, RNI and FNI reduce errors by 1.06 and 1.12, which indicates that the motion priors can enhance movement consistency with the source video.

**Threshold of residual-based noise initialization.** We analyze the effects of three types of initial noise: identical noise (threshold=1.0), distinct noise (threshold=0.0), and motion-enhanced noise (threshold=0.1). It is important to note that this threshold also regulates the smoothness of the resulting video. As shown in Figure 8, in the second row, when there is no residual control, the background is prone to flickering, such as water color. The third row corresponds to the threshold we select, which effectively balances consistency and smoothness to produce satisfactory results. The final row displays the consequence of using the same noise for each frame, a smooth video, but with severe artifacts. Overall, incorporating residual-based noise can introduce motion from the input video, resulting in videos with reduced flickering and better consistency.

### 4.3.2 Latent First-frame Conditioned Controller

Our first-frame conditioning strategy provides content priors for video generation, encouraging subsequent frames to keep object consistency with the first frame. Because the initial frame from text-to-image process can achieve high quality and text-aligned easily, two-stage video generation facilitates semantic alignment with prompt compared with generating an entire video directly. Figure 9 compares the results with and without the first-frame conditioning strategy. In this case, the caption describes the bus is red and blue, but the result without first-frame conditioning pro-

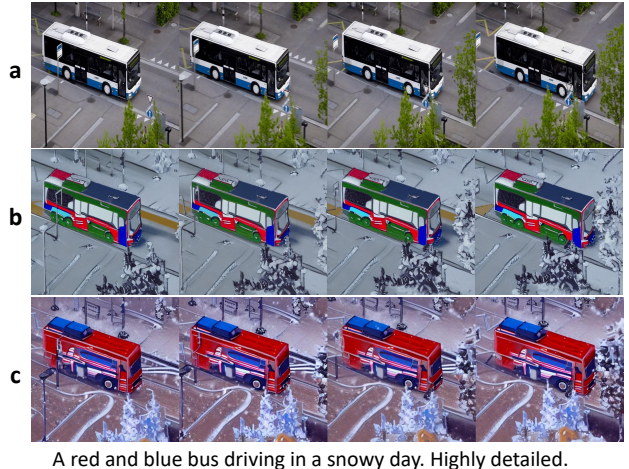


Figure 9. Qualitative ablation study of the first-frame conditioned controller (FFC). (a) Input video, (b) Ours w/o FFC, (c) Ours with FFC.

type	text	frame	depth	optical flow
baseline	0.238	0.950	0.149	4.78
+ FFC	0.262	0.964	0.086	4.40
+ RNI	0.256	0.954	0.104	3.72
+ FNI	0.255	0.954	0.095	3.66
+ FFC + RNI	0.264	0.960	0.092	4.12
+ FFC + FNI	0.261	0.965	0.088	4.09

Table 1. Quantitative comparison for our strategies in terms of text alignment, frame similarity, depth map error and optical flow map error. The baseline indicates the model trained with depth maps as control. FFC means first-frame conditioned controller. RNI and FNI correspond to pixel residual-based and optical flow-based noise initialization.

duces a bus in wrong color. Moreover, our model can generate snowflakes in the video background, which is consistent with “a snowy day”. According to Table 1, the first-frame conditioned controller brings boost in text alignment, from 0.238 to 0.262, and reduces depth errors, from 0.149 to 0.086, over the baseline. Compared with noise initialization strategies, first-frame conditioning plays a more important role in text alignment and depth consistency.

## 5. Conclusion

In this paper, we propose a controllable T2V framework that is capable of generating videos conditioned on text prompts and control maps. With the proposed motion-adaptive noise initialization and first-frame conditioning strategies, we introduce motion priors and content priors to promote video consistency. After temporal learning in a small video dataset, our model can generate coherent, text-aligned, long videos. While our method achieves impressive results, it still has some known limitations. For ex-

ample, our T2V model relies on a T2I model and shares the same bad cases. In the future, it’s worth conducting research on the stability and controllability of the video generation models.

## References

- [1] Andreas Blattmann, Robin Rombach, Huan Ling, Tim Dockhorn, SeungWook Kim, Sanja Fidler, and Karsten Kreis. Align your latents: High-resolution video synthesis with latent diffusion models. 2023. [2](#), [3](#)
- [2] Tim Brooks, Aleksander Holynski, and Alexei A Efros. Instructpix2pix: Learning to follow image editing instructions. *arXiv preprint arXiv:2211.09800*, 2022. [3](#)
- [3] John Canny. A computational approach to edge detection. *IEEE Transactions on Pattern Analysis and Machine Intelligence*, page 679–698, 2009. [6](#)
- [4] Patrick Esser, Johnathan Chiu, Parmida Atighehchian, Jonathan Granskog, and Anastasis Germanidis. Structure and content-guided video synthesis with diffusion models. *arXiv preprint arXiv:2302.03011*, 2023. [2](#), [3](#), [6](#), [7](#)
- [5] Rinon Gal, Yuval Alaluf, Yuval Atzmon, Or Patashnik, Amit H Bermano, Gal Chechik, and Daniel Cohen-Or. An image is worth one word: Personalizing text-to-image generation using textual inversion. *arXiv preprint arXiv:2208.01618*, 2022. [3](#)
- [6] Songwei Ge, Seungjun Nah, Nvidia Guilin, Liu Nvidia, Tyler Poon, Andrew Tao Nvidia, Bryan Catanzaro, Jia-Bin Huang, Ming-Yu Liu, Nvidia Yogesh, and Balaji Nvidia. Preserve your own correlation: A noise prior for video diffusion models. [2](#)
- [7] Michal Geyer, Omer Bar-Tal, Shai Bagon, and Tali Dekel. Tokenflow: Consistent diffusion features for consistent video editing. 2023. [3](#), [7](#)
- [8] Ian Goodfellow, Jean Pouget-Abadie, Mehdi Mirza, Bing Xu, David Warde-Farley, Sherjil Ozair, Aaron Courville, and Yoshua Bengio. Generative adversarial networks. *Communications of the ACM*, 63(11):139–144, 2020. [3](#)
- [9] Yuwei Guo, Ceyuan Yang, Anyi Rao, Yaohui Wang, Yu Qiao, Dahua Lin, and Bo Dai. Animatediff: Animate your personalized text-to-image diffusion models without specific tuning. 2023. [3](#)
- [10] Yingqing He, Tianyu Yang, Yong Zhang, Ying Shan, and Qifeng Chen. Latent video diffusion models for high-fidelity video generation with arbitrary lengths. 2022. [3](#)
- [11] Amir Hertz, Ron Mokady, Jay Tenenbaum, Kfir Aberman, Yael Pritch, and Daniel Cohen-Or. Prompt-to-prompt image editing with cross attention control. *arXiv preprint arXiv:2208.01626*, 2022. [3](#)
- [12] Jonathan Ho and Tim Salimans. Classifier-free diffusion guidance. [6](#)
- [13] Jonathan Ho, Ajay Jain, and Pieter Abbeel. Denoising diffusion probabilistic models., 2020. [3](#), [1](#)
- [14] Jonathan Ho, William Chan, Chitwan Saharia, Jay Whang, Ruiqi Gao, Alexey Gritsenko, Diederik P Kingma, Ben Poole, Mohammad Norouzi, David J Fleet, et al. Imagen video: High definition video generation with diffusion models. *arXiv preprint arXiv:2210.02303*, 2022. [3](#)
- [15] Jonathan Ho, Tim Salimans, Alexey Gritsenko, William Chan, Mohammad Norouzi, and David J Fleet. Video diffusion models. *arXiv preprint arXiv:2204.03458*, 2022. [3](#)
- [16] Lianghua Huang, Di Chen, Yu Liu, Yujun Shen, Deli Zhao, and Jingren Zhou. Composer: Creative and controllable image synthesis with composable conditions. 2023. [3](#)
- [17] Levon Khachatryan, Andranik Movsisyan, Vahram Tadevosyan, Roberto Henschel, Zhangyang Wang, Shant Navasardyan, and Humphrey Shi. Text2video-zero: Text-to-image diffusion models are zero-shot video generators. *arXiv preprint arXiv:2303.13439*, 2023. [2](#), [3](#), [7](#)
- [18] Diederik P. Kingma and Max Welling. Auto-encoding variational bayes. *arXiv: Machine Learning, arXiv: Machine Learning*, 2013. [3](#)
- [19] Junnan Li, Dongxu Li, Caiming Xiong, and Steven Hoi. Blip: Bootstrapping language-image pre-training for unified vision-language understanding and generation. [4](#)
- [20] Shaoteng Liu, Yuechen Zhang, Wenbo Li, Zhe Lin, and Jiaya Jia. Video-p2p: Video editing with cross-attention control. 2023. [3](#)
- [21] Chong Mou, Xintao Wang, Liangbin Xie, Jian Zhang, Zhonggang Qi, Ying Shan, and Xiaohu Qie. T2i-adapter: Learning adapters to dig out more controllable ability for text-to-image diffusion models. *arXiv preprint arXiv:2302.08453*, 2023. [3](#)
- [22] Bolin Ni, Houwen Peng, Minghao Chen, Songyang Zhang, Gaofeng Meng, Jianlong Fu, Shiming Xiang, and Haibin Ling. Expanding language-image pretrained models for general video recognition, 2022. [7](#)
- [23] Alex Nichol, Prafulla Dhariwal, Aditya Ramesh, Pranav Shyam, Pamela Mishkin, Bob McGrew, Ilya Sutskever, and Mark Chen. Glide: Towards photorealistic image generation and editing with text-guided diffusion models. [2](#), [3](#)
- [24] Hao Ouyang, Qiuyu Wang, Yuxi Xiao, Qingyan Bai, Juntao Zhang, Kecheng Zheng, Xiaowei Zhou, Qifeng Chen, and Yujun Shen. Codef: Content deformation fields for temporally consistent video processing. *arXiv preprint arXiv:2308.07926*, 2023. [3](#)
- [25] Jordi Pont-Tuset, Federico Perazzi, Sergi Caelles, Pablo Arbeláez, Alexander Sorkine-Hornung, and Luc Van Gool. The 2017 davis challenge on video object segmentation, 2017. [7](#)
- [26] Chenyang Qi, Xiaodong Cun, Yong Zhang, Chenyang Lei, Xintao Wang, Ying Shan, and Qifeng Chen. Fatezero: Fusing attentions for zero-shot text-based video editing. *arXiv preprint arXiv:2303.09535*, 2023. [2](#), [3](#)
- [27] Aditya Ramesh, Prafulla Dhariwal, Alex Nichol, Casey Chu, and Mark Chen. Hierarchical text-conditional image generation with clip latents. [2](#), [3](#), [6](#)
- [28] Rene Ranftl, Katrin Lasinger, David Hafner, Konrad Schindler, and Vladlen Koltun. Towards robust monocular depth estimation: Mixing datasets for zero-shot cross-dataset transfer. *IEEE Transactions on Pattern Analysis and Machine Intelligence*, page 1623–1637, 2020. [6](#)
- [29] Nataniel Ruiz, Yuanzhen Li, Varun Jampani, Yael Pritch, Michael Rubinstein, and Kfir Aberman. Dreambooth: Fine tuning text-to-image diffusion models for subject-driven generation, 2022. [3](#)

- [30] Chitwan Saharia, William Chan, Saurabh Saxena, Lala Li, Jay Whang, Emily L Denton, Kamyar Ghasemipour, Raphael Gontijo Lopes, Burcu Karagol Ayan, Tim Salimans, et al. Photorealistic text-to-image diffusion models with deep language understanding. *Advances in Neural Information Processing Systems*, 35:36479–36494, 2022. [2](#), [3](#)
- [31] Christoph Schuhmann, Romain Beaumont, Richard Vencu, Cade Gordon, Ross Wightman, Mehdi Cherti, Theo Coombes, Aarush Katta, Clayton Mullis, Mitchell Wortsman, Patrick Schramowski, Srivatsa Kundurthy, Katherine Crowson, Ludwig Schmidt, Robert Kaczmarczyk, and Jenia Jitsev. Laion-5b: An open large-scale dataset for training next generation image-text models, 2022. [6](#)
- [32] Uriel Singer, Adam Polyak, Thomas Hayes, Xi Yin, Jie An, Songyang Zhang, Qiyuan Hu, Harry Yang, Oron Ashual, Oran Gafni, et al. Make-a-video: Text-to-video generation without text-video data. *arXiv preprint arXiv:2209.14792*, 2022. [3](#)
- [33] Jiaming Song, Chenlin Meng, and Stefano Ermon. Denoising diffusion implicit models, 2020. [3](#)
- [34] Narek Tumanyan, Michal Geyer, Shai Bagon, and Tali Dekel. Plug-and-play diffusion features for text-driven image-to-image translation. *arXiv preprint arXiv:2211.12572*, 2022. [3](#)
- [35] Vikram Voleti, Alexia Jolicoeur-Martineau, Christopher Pal, Polytechnique Montréal, Canada Cifar, AI Chair, and Servicenow Research. Masked conditional video diffusion for prediction, generation, and interpolation. [3](#)
- [36] Wen Wang, Kangyang Xie, Zide Liu, Hao Chen, Yue Cao, Xinlong Wang, and Chunhua Shen. Zero-shot video editing using off-the-shelf image diffusion models. [3](#)
- [37] Xiang Wang, Hangjie Yuan, Shiwei Zhang, Dayou Chen, Junyi Wang, Yingya Zhang, Yujun Shen, Deli Zhao, and Jingren Zhou. Videocomposer: Compositional video synthesis with motion controllability. 2023. [2](#), [3](#), [7](#)
- [38] Jay Zhangjie Wu, Yixiao Ge, Xintao Wang, Weixian Lei, Yuchao Gu, Wynne Hsu, Ying Shan, Xiaohu Qie, and Mike Zheng Shou. Tune-a-video: One-shot tuning of image diffusion models for text-to-video generation. *arXiv preprint arXiv:2212.11565*, 2022. [3](#)
- [39] Saining Xie and Zhuowen Tu. Holistically-nested edge detection. In *2015 IEEE International Conference on Computer Vision (ICCV)*, 2016. [6](#)
- [40] Jinbo Xing, Menghan Xia, Yuxin Liu, Yuechen Zhang, Yong Zhang, Yingqing He, Hanyuan Liu, Haoxin Chen, Xiaodong Cun, Xintao Wang, Ying Shan, and Tien-Tsin Wong. Make-your-video: Customized video generation using textual and structural guidance. *CoRR*, abs/2306.00943, 2023. [2](#)
- [41] Shuai Yang, Yifan Zhou, Ziwei Liu, and ChenChange Loy. Rerender a video: Zero-shot text-guided video-to-video translation. [2](#), [3](#), [7](#)
- [42] Lvmin Zhang and Maneesh Agrawala. Adding conditional control to text-to-image diffusion models. *arXiv preprint arXiv:2302.05543*, 2023. [2](#), [3](#), [6](#)



# Control-A-Video: Controllable Text-to-Video Generation with Diffusion Models

## Supplementary Material

### A. Preliminary

**Diffusion Models:** Given an input signal  $x_0$ , a diffusion forward process is defined as:

$$p_\theta(x_t|x_{t-1}) = \mathcal{N}(x_t; \sqrt{1 - \beta_{t-1}}x_{t-1}, \beta_t I), \quad t = 1, \dots, T \quad (8)$$

where  $T$  is the total timestep of the diffusion process. A noise depending on variance  $\beta_t$  is gradually added to  $x_{t-1}$  to obtain  $x_t$  at the next timestep and finally reach  $x_T \in \mathcal{N}(0, I)$ . The goal of the diffusion model [13] is to learn to reverse the diffusion process (denoising). Given a random noise  $x_t$ , the model predicts the added noise at the next timestep  $x_{t-1}$  until the origin signal  $x_0$ .

$$p_\theta(x_{t-1}|x_t) = \mathcal{N}(x_{t-1}; \mu_\theta(x_t, t), \Sigma_\theta(x_t, t)), \quad t = T, \dots, 1 \quad (9)$$

We fix the variance  $\Sigma_\theta(x_t, t)$  and utilize the diffusion model with parameter  $\theta$  to predict the mean of the inverse process  $\mu_\theta(x_t, t)$ . The model can be simplified as denoising models  $\epsilon_\theta(x_t, t)$ , which are trained to predict the noise of  $x_t$  with a noise prediction loss:

$$\min_\theta \|\epsilon - \epsilon_\theta(x_t, t, c_p)\|_2^2 \quad (10)$$

where  $\epsilon$  is the added noise to the input image  $x_0$ , the model learn to predict the noise of  $x_t$  conditioned on text prompt  $c_p$  at timestep  $t$ .

**Latent diffusion Models:** LDM propose to apply a compressed latent code  $z$  rather than the image signal  $x$  in diffusion process to speed up the denoising process. The image  $x$  is encoded by an encoder  $\mathcal{E}$  to obtain the latent code  $z = \mathcal{E}(x)$ , and the model learns to denoise in latent space. During inference, the reconstructed latent code  $z_0$  can be reconstructed by a decoder  $\mathcal{D}$ ,  $x_0 = \mathcal{D}(z_0)$  to obtain the generated image.

**ControlNet:** ControlNet is a neural network architecture that enhances pretrained image diffusion models with task-specific conditions by utilizing trainable layers copied from the original diffusion model. These layers are then fine-tuned based on specific control maps such as edge, depth, and segmentation inputs. The loss with additional control can be formulated as:

$$\min_\theta \|\epsilon - \epsilon_\theta(x_t, t, c_p, c_f)\|_2^2 \quad (11)$$

where the control map  $c_f$  is an additional control. Our research draws inspiration from ControlNet and expands its application into video synthesis. In the case of a video, the input signal  $x$  and control  $c_f$  is extended to a sequence of  $N$  frames.

### B. More Experiment results

#### B.1. Cases show

Please refer to the uploaded video in the attachment, which includes a majority of the videos referenced in this paper, along with additional cases. The video can also be downloaded from this [link](#). **(1) Practical Usage Cases:** We explore the practical applications of our model in the field of video editing. These videos are generated using an autoregressive approach, often repeated two or three times such as Figure 5, as an exciting bonus feature resulting from our innovative frame-condition strategy. **(2) Support for Different Control Maps:** We provide more cases than Figure 1 to demonstrate the versatility of our model in supporting various control maps as conditions. Depth control offers enhanced flexibility, allowing for more creative freedom, while edge control ensures greater consistency in the edited videos. **(3) Ablation Study for Motion Prior:** We conduct an in-depth ablation study focusing on motion prior. By training and inferring the model with different noise priors, we validate the effectiveness of our proposed motion-guided noise technique, showcasing its impact on the generated videos as Figure 7. **(4) Ablation Study for Latent First-Frame Conditioned Controller:** We present an ablation study where videos are generated by conditioning the model on an image from a Text-to-Image (T2I) model, such as Figure 9. This approach improves text alignment and enhances the overall quality of the generated videos. **(5) Ablation Study with Varying Thresholds for Residual-Based Noise:** We conduct an additional ablation study as Figure 8, exploring the effects of different thresholds for residual-based noise. This analysis helps us better understand the impact of noise on the generated videos. **(6) Comparison with Other Methods:** In the final section, we conduct a comprehensive comparison between our proposed method and other existing approaches in the field of video editing as Figure 6. This analysis aims to highlight the unique advantages of our model and its potential for advancing the current state-of-the-art techniques.

#### B.2. Quantitative Comparison

**Training Resources Comparison.** We evaluate the training expense based on the total number of iterations performed on training samples, which can be computed as  $\text{batchsize} \times \text{trainingsteps}$ . As presented in Table 2, we require roughly 1000x less iteration steps of samples compared to Gen-1's. Moreover, we make a comparison of the dataset capacity and find that we employ 240x fewer images and 64x fewer videos than their dataset. The model

Type	BS	step	image num	video num
Gen-1	1192	115k	240M	6.4M
Ours	16	10k	100k	100k

Table 2. Comparison of training resources. ‘BS’ and ‘step’ indicate batch size and step number of training.

can be trained with 16 A100 with batch size 16 in 12 hours, and we believe it will achieve better result if we scale up the data. We demonstrate that we achieve competitive text-coherent results and better consistency with such less training resources with the proposed methods.

**Quantitative Comparison.** We conduct comparison with other end-to-end models on the videos used in Section 4.3. We choose three typical models, including Gen-1 that is trained for video editing, Text2video-zero performing zero-shot video editing, and Video Composer which is a controllable video generation method. As shown in Table 3, our model achieves the best results.

Type	text $\uparrow$	depth $\downarrow$	flow $\downarrow$
Gen-1 <sup>1</sup> [4]	0.252	0.112	6.16
T2V-Zero [17]	0.249	0.139	4.99
Composer [37]	0.259	0.104	4.23
Ours	0.261	<b>0.088</b>	4.09

Table 3. Comparison of quantitative result with existing methods for T2V conditioned on depth maps in terms of text alignment and consistency.

### B.3. User Study

18 participants were surveyed to evaluate the textual alignment and consistency of the generated videos with human-written prompts by utilizing a rating scale ranging from 1 to 5. The data presented in Table 4 indicates that our model yields videos that demonstrate greater consistency aligned the quantity result of depth error findings, with the text alignment score exhibiting comparable results.

Type	Text Align $\uparrow$	Consistency $\uparrow$
Gen-1 [4]	4.25	3.89
Text2Video-Zero [17]	3.68	3.21
Video-Composer [37]	3.98	3.63
Ours	4.08	<b>4.18</b>

Table 4. Comparison of user study with existing methods for T2V conditioned on depth maps in terms of text alignment and consistency.

<sup>1</sup>We utilize Gen-1 website to produce video results, which contain some post-process operations, including frame interpolation. Therefore, we have to select some frames corresponding to original inputs, which may bring errors to some extent.

### B.4. Ablation study of our model structure

In Figure 10, we conduct a visualization ablation to showcase the effect of spatial-temporal attention and training. We present some video generation results with the spatial-temporal attention and pixel residual-based noise initializer in a zero-shot manner. As shown in Figure 10, the video of the second row is generated without any strategies and is totally inconsistent; the third row is using the proposed spatial-temporal attention that becomes more content-consistent but flickering (you should have a look at the video in supplementary material to tell the difference); the fourth row is less flickering than the third one since the residual can introduce the motion priors and improve consistency; the last row is the result after training the model with our proposed methods, which is really consistent. In conclusion, after applying the proposed methods, the model can generate somewhat consistent videos. However, it’s necessary to have a further temporal learning process to get more consistent results without flickering.



Figure 10. The prompt is ‘a bear walking through stars’. We demonstrate the ability of our proposed spatial-temporal attention and residual motion prior in both zero-shot and training setting.